Developmental Cognitive Neuroscience 24 (2017) 107–117

Contents lists available at ScienceDirect

Developmental Cognitive Neuroscience

journal homepage: http://www.elsevier.com/locate/dcn

The neural and behavioral correlates of social evaluation in childhood

Michelle Achterberg[a,b,c,*], Anna C.K. van Duijvenvoorde[a,b,c], Mara van der Meulen[a,b,c], Saskia Euser[a,d], Marian J. Bakermans-Kranenburg[a,c,d], Eveline A. Crone[a,b,c]

[a] Leiden Consortium on Individual Development, Leiden University, The Netherlands
[b] Institute of Psychology, Leiden University, The Netherlands
[c] Leiden Institute for Brain and Cognition, Leiden University, The Netherlands
[d] Centre for Child and Family Studies, Leiden University, The Netherlands

ARTICLE INFO

Article history:
Received 2 August 2016
Received in revised form 16 February 2017
Accepted 17 February 2017
Available online 27 February 2017

Keywords:
Social feedback
Social rejection
Aggression
Childhood
Amygdala
Meta-analysis

ABSTRACT

Being accepted or rejected by peers is highly salient for developing social relations in childhood. We investigated the behavioral and neural correlates of social feedback and subsequent aggression in 7–10-year-old children, using the Social Network Aggression Task (SNAT). Participants viewed pictures of peers that gave positive, neutral or negative feedback to the participant's profile. Next, participants could blast a loud noise towards the peer, as an index of aggression. We included three groups ($N = 19$, $N = 28$ and $N = 27$) and combined the results meta-analytically. Negative social feedback resulted in the most behavioral aggression, with large combined effect-sizes. Whole brain condition effects for each separate sample failed to show robust effects, possibly due to the small samples. Exploratory analyses over the combined test and replication samples confirmed heightened activation in the medial prefrontal cortex (mPFC) after negative social feedback. Moreover, meta-analyses of activity in predefined regions of interest showed that negative social feedback resulted in more neural activation in the amygdala, anterior insula and the mPFC/anterior cingulate cortex. Together, the results show that social motivation is already highly salient in middle childhood, and indicate that the SNAT is a valid paradigm for assessing the neural and behavioral correlates of social evaluation in children.

1. Introduction

Social acceptance is of key importance in life. Receiving positive social feedback increases our self-esteem and gives us a sense of belonging (Thomaes et al., 2011). Receiving negative social feedback, in contrast, can induce feelings of depression, and rejected people often react with withdrawal (Nolan et al., 2003). Social rejection can, however, also trigger feelings of anger and frustration, and can lead to reactive aggressive behavior (Dodge et al., 2003; Nesdale and Lambert, 2007; Chester et al., 2014; Riva et al., 2015; Achterberg et al., 2016). Most developmental studies have focused on the withdrawal reaction after social rejection, while relatively few have examined reactive aggression. The few studies that examined rejection-related aggression showed that early peer rejection was associated with an increase in aggression in children aged 6–8 (Dodge et al., 2003; Lansford et al., 2010). Several prior studies have also shown that rejection can lead to immediate aggression (Chester et al., 2014; Riva et al., 2015; Achterberg et al., 2016). These immediate effects may be associated with emotional responses to rejection and a lack of impulse control. Although several studies have focused on neural processes involved in negative versus positive social feedback processing, the neural processes involved in dealing with negative or positive social feedback versus a neutral baseline in middle childhood are currently unknown.

Experimental research in adults has examined social evaluation and aggression using a peer acceptance and rejection task. Initially developed as a social feedback task (Somerville et al., 2006), a recent adaptation allowed participants to deliver noise blasts to peers who had rejected them based on a personal profile (Achterberg et al., 2016), testing the potential expression of reactive aggression. Negative social feedback signaling rejection was associated with louder noise blasts and increased activity in bilateral anterior insula and medial prefrontal cortex (mPFC)/anterior cingulate cortex (ACC) relative to neutral feedback (Achterberg et al., 2016). This latter region is suggested to play an important role in evaluating others' behaviors and in estimating others' level of motivation (Flagan and Beer, 2013; Apps et al., 2016). Interestingly, these regions were also more active after positive feedback (compared to neutral feedback), suggesting that both negative and positive feedback leads to social evaluative processes in adults. Other studies also reported the involvement of subcortical regions in processing social feedback.

* Corresponding author at: Faculty of Social Sciences, Leiden University, Wassenaarseweg 52, 2333AK Leiden, The Netherlands.
E-mail address: m.achterberg@fsw.leidenuniv.nl (M. Achterberg).

http://dx.doi.org/10.1016/j.dcn.2017.02.007

Positive social feedback was found to result in greater activity in striatal regions (Gunther Moor et al., 2010; Achterberg et al., 2016), which possibly reflects the rewarding value of this type of feedback (Guyer et al., 2014). Furthermore, peer interactions have been associated with increased amygdala activity, indicating their affective salience (Guyer et al., 2008; Masten et al., 2009; Silk et al., 2014).

Several studies examined the neural correlates of social evaluation in children and adolescents. These studies reported increased neural activity to positive relative to negative feedback in older adolescents and adults (16–25) as indicated by increased activity in the ventral mPFC, the subcallosal cortex, and the ACC (Gunther Moor et al., 2010). Another study found increased pupil dilation in response to social rejection (compared to acceptance) in children aged 9–17 (Silk et al., 2012a). Pupil dilation is an index of increased activity in cognitive and affective processing regions of the brain, such as the ACC and amygdala (Silk et al., 2012a), and the pupil becomes more dilated in response to stimuli with a greater emotional intensity (Siegle et al., 2003). Interestingly, the pupil dilation effect was larger for older participants, indicating that adolescents reacted more strongly to rejection than children. The current study examined the neural correlates of social evaluation in middle childhood, prior to adolescence, because the first long-lasting friendships gradually emerge around this time (Berndt, 2004). Furthermore, we tested whether peer rejection in children results in behavioral aggression, in a similar way as was previously observed in adults (Chester et al., 2014; Riva et al., 2015; Achterberg et al., 2016).

Thus, our aim was to investigate 7–10-year-old children's responses to social evaluation in terms of neural activity and reactive behavioral aggression. For this purpose, we used the Social Network Aggression Task (SNAT), that elicited robust neural and behavioral responses in adults (Achterberg et al., 2016), but has not yet been used with children. During the SNAT, participants viewed pictures of peers who gave positive, neutral or negative feedback to the participant's profile. Next, participants could deliver an imagined noise blast towards the peer, as an index of (imagined) aggression or frustration. Since recent studies have reported concerns about the replicability of psychological science (for example see Open Science (2015)), we used three samples to validate the paradigm: a pilot sample, a test sample, and a replication sample. Moreover, findings that may show no evidence of significance when analyzed individually might provide stronger evidence when collapsed across experiments, as was recently shown (Scheibehenne et al., 2016). Therefore we also include a meta-analytic combination of the results across the three samples.

On the behavioral level we expected that the pattern of aggression after positive, neutral, and negative feedback would be similar across the pilot, test and replication samples, with negative feedback resulting in the highest levels of aggressive behavior. On the neural level we examined both the general contrast of social evaluation (all feedback conditions vs. baseline; see Supplementary materials) and the condition-specific contrasts. To further investigate condition effects, that is the effect of negative *vs*. neutral *vs*. positive feedback, we used regions of interest (ROI) analyses. The individual ROI analyses were meta-analytically combined in order to test for robust condition effects across our samples. Based on studies in adults, the predictions were that negative social feedback would be associated with increased activity in the amygdala (Masten et al., 2009), bilateral insula, and mPFC/Anterior Cingulate Cortex' gyrus ACCg (Somerville et al., 2006; Achterberg et al., 2016). While prior studies tested only adults and adolescents, this study tested for the first time if the same regions are engaged in children, including not only positive and negative social feedback but also a neutral social feedback baseline (see Achterberg et al., 2016), and examined the relations with subsequent aggression.

Table 1
Demographic characteristics of the samples.

	Pilot	Test	Replication
N	19	28	27
% boys	53%	43%	44%
Left handed	none	3	6
AXIS-I disorder	none	none	1 (ADHD)
Mean Age (SD)	8.18 (0.97)	8.23 (0.67)	8.28 (0.65)
Age Range	7.20–10.99	7.03–8.97	7.03–8.97
Mean IQ (SD)	102.76 (11.54)	101.57 (12.33)	104.54 (10.58)
IQ range	85.00–127.50	77.50–125.00	85.00–132.50

2. Materials and methods

2.1. Participants

Participants in this study were part of the larger, longitudinal twin study of the Leiden Consortium on Individual Development (L-CID). Families with a twin born between 2006 and 2009, living within two hours travel time from Leiden, were recruited through the Dutch municipal registry and received an invitation to participate by post. Parents could show their interest in participation using a reply card. For the larger L-CID study, only same-sex twins were included. Opposite-sex twins were included only in the pilot study. The pilot sample consisted of 20 children between the ages of 7 and 10 (11 boys, $M = 8.16$ years, $SD = 0.95$), including 9 opposite-sex twin pairs. Two additional participants were recruited from a participant data base at Leiden University. Two months after the pilot sample, the test and replication samples were recruited. The test and replication sample consisted of 30 same-sex twin pairs (16 boys, $M = 8.22$ years, $SD = 0.67$), including 7 monozygotic pairs. After data collection, but prior to data analyses, first and second born children (within the twin pair) were randomly assigned to the test and replication sample. For a schematic overview of sample selection see Fig. S1 (Supplementary materials). The Dutch Central Committee on Human Research (CCMO) approved the study and its procedures. Written informed consent was obtained from both parents. All participants were fluent in Dutch, had normal or corrected-to-normal vision, and were screened for MRI contra indications. All anatomical MRI scans were reviewed and cleared by a radiologist from the radiology department of the Leiden University Medical Center (LUMC). No anomalous findings were reported.

Six participants were excluded due to excessive head motion, which was defined as >1 mm movement in >20% of the volumes (one from the pilot sample, two from the test sample and three from the replication sample). The final pilot sample consisted of 19 participants, including 8 twin pairs (10 boys, $M = 8.18$ years, $SD = 0.97$), the final test sample consisted of 28 participants (12 boys, $M = 8.23$ years, $SD = 0.67$) and the final replication sample consisted of 27 participants (12 boys, $M = 8.28$ years, $SD = 0.65$). Demographics of the final samples are listed in Table 1. Participants' intelligence (IQ) was estimated with the subsets 'similarities' and 'block design' of the Wechsler Intelligence Scale for Children, third edition (WISC-III; Wechsler, 1997). For all three samples, estimated IQs were in the normal to high range (see Table 1). In all three samples, IQ scores were unrelated to behavioral outcomes of the SNAT (noise blast duration after positive, neutral, negative feedback, all p's > 0.214).

2.2. Social network aggression task

The Social Network Aggression Task (SNAT) as described in Achterberg et al. (2016) was used to measure (imagined) aggression after social evaluation. The task was programmed in Eprime (version 2.0.10.356). Prior to the fMRI session, the children filled in a personal profile at home, which was handed in at least one week

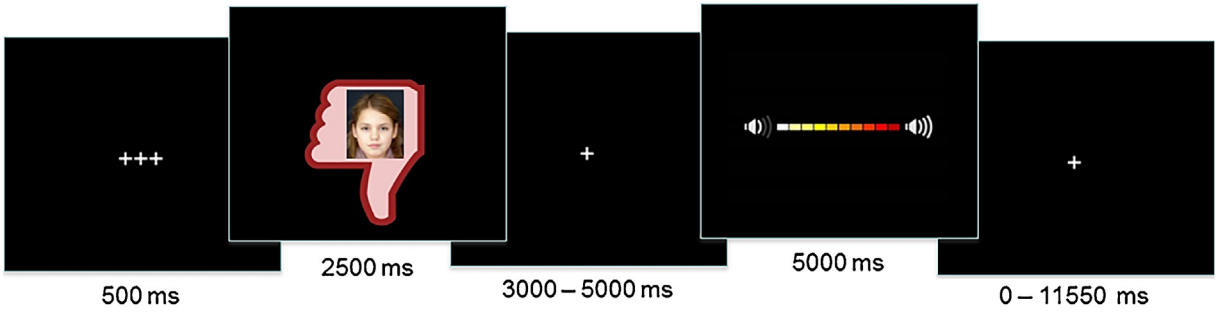

Fig. 1. Display of one trial of the Social Network Aggression Task (SNAT).

before the actual fMRI session. The profile page consisted of questions such as: *'What is your favorite movie?'*, *'What is your favorite sport?'*, and *'What is your biggest wish?'*. Children were informed that their profiles were reviewed by other, unfamiliar, children. During the SNAT the children were presented with pictures and feedback from same-aged peers in response to their personal profile. Every trial consisted of feedback from a new unfamiliar child. This feedback could either be positive ('I like your profile', or 'I like the same movies and the same sports', visualized by a green thumb up); negative ('I do not like your profile', or 'I hate your sport and don't like that movie'; red thumb down) or neutral ('I don't know what to think of your profile', or 'I like your sport, but hate that movie', grey circle). Following each peer feedback, the children were instructed to imagine that they could send a loud noise blast to this peer. We specifically instructed the children to imagine this to reduce deception, and studies showed that imagined play also leads to aggression (Konijn et al., 2007). The longer they pressed the button the more intense the noise would be, which was visually represented by a volume bar (Fig. 1). To keep task demands as similar as possible between the conditions, participants were instructed to always press the button, but they could choose whether they wanted a short noise at low intensity or a long noise at high intensity. Unbeknownst to the participants, others did not judge the profile, and the photos were created by morphing two children of an existing data base (matching the age range) into a new, non-existing child. Peer pictures were randomly coupled to feedback, ensuring equal gender proportions for each type of feedback. Deception was assessed using an exit interview with open questions, such as 'what did you think of the game', and 'what did you think of the noises that you could delivered'. None of the participants expressed doubts about the cover story.

Participants were familiarized with the MRI scanner with a practice session in a mock scanner. Then participants received instructions on how to perform the SNAT and the children were exposed to the noise blast twice during a practice session: once with stepwise build-up of intensity and once at maximum intensity. Participants did not hear the noise during the fMRI session, to prevent that pressing the button would punish the participants themselves. To familiarize participants with the task, participants performed six practice trials. After the practice session, one of the twins continued with the actual scanning session, while the other twin performed the WISC-III and other behavioral tasks. First-born and second-born children were randomly assigned to the scan session or behavioral session as their first task. When the first child completed the scanning session, he/she continued with the WISC-III and behavioral tasks while the other child participated in the scanning session.

The SNAT consisted of 60 trials, three blocks of 20 trials for each social feedback condition (positive, neutral, negative), that were presented semi-randomized to ensure that no condition was presented more than three times in a row. The first block consisted of 7 positive, 6 neutral, and 7 negative feedback trials; the second block consisted of 8 positive, 6 neutral, 6 negative feedback trials; and the third block consisted of 5 positive, 8 neutral, and 7 negative feedback trials. The optimal jitter timing and order of events were calculated with Optseq 2 (Dale, 1999). Each trial started with a fixation screen (500 ms), followed by the social feedback (2500 ms). After another jittered fixation screen (3000–5000 ms), the noise screen with the volume bar appeared, which was presented for a total of 5000 ms. Children were instructed to deliver the noise blast by pressing one of the buttons on the button box attached to their legs, with their right index finger. As soon as the participant started the button press, the volume bar started to fill up with a newly colored block appearing every 350 ms. After releasing the button, or at maximum intensity (after 3500 ms), the volume bar stopped increasing and stayed on the screen for the remainder of the 5000 ms. Before the start of the next trial, another jittered fixation cross was presented (0–11550 ms) (Fig. 1). The length of the noise blast duration (i.e., length of button press) was used as a measure of aggression.

2.3. MRI data acquisition

MRI scans were acquired with a standard whole-head coil on a Philips 3.0 T scanner. The data of the pilot sample were collected on a Philips Achieva TX MR system, the data of the test and replication sample were collected on a Philips Ingenia MR system. To prevent head motion, foam inserts surrounded the children's heads. The SNAT was projected on a screen that was viewed through a mirror on the head coil. Functional scans were collected during three runs T2*-weighted echo planar images (EPI). The first two volumes were discarded to allow for equilibration of T1 saturation effect. Volumes covered the whole brain with a field of view (FOV) = 220 (ap) × 220 (rl) × 111.65 (fh) mm; repetition time (TR) of 2.2 s; echo time (TE) = 30 ms; flip angle (FA) = 80°; sequential acquisition, 37 slices; and voxel size = 2.75 × 2.75 × 2.75 mm. In the pilot sample the FOV was 220 (ap) × 220 (rl) × 114.68 (fh) mm, with a sequential acquisition of 38 slices. All other parameters were equal. Subsequently, a high-resolution 3D T1scan was obtained as anatomical reference (FOV = 224 (ap) × 177 (rl) × 168 (fh); TR = 9.72 ms; TE = 4.95 ms; FA = 8°; 140 slices; voxel size 0.875 × 0.875 × 0.875 mm). In the pilot sample the TR = 9.79 and the TE = 4.60, all other parameters were equal.

2.4. MRI data analyses

2.4.1. Preprocessing

MRI data were analyzed with SPM8 (Wellcome Trust Centre for Neuroimaging, London). Images were corrected for slice timing acquisition and rigid body motion. Functional scans were spatially normalized to T1 templates. Volumes of all children were resampled to 3 × 3 × 3 mm voxels. Data were spatially smoothed with a

6 mm full width at half maximum (FWHM) isotropic Gaussian kernel. SPM8's ARTrepair toolbox (Mazaika et al., 2009) was used to detect and fix bad slices in preprocessed functional data. Slices with >1 mm scan to scan motion were detected and repaired. Children with >20% repaired slices were excluded from further analyses.

2.4.2. First-level analyses

Statistical analyses were performed on individual subjects' data using a general linear model. The fMRI time series were modeled as a series of two events convolved with the hemodynamic response function (HRF). The onset of social feedback was modeled as the first event with a zero duration and with separate regressors for the positive, negative, and neutral peer feedback. The start of the noise blast was modeled for the length of the noise blast duration (i.e., length of button press) and with separate regressors for noise blast after positive, negative, and neutral feedback. Trials on which the participants failed to respond in time were modeled separately as covariate of no interest and were excluded from further analyses. On average 7.3% of the trials were invalid (pilot: 7.8%, test: 7.3%, replication: 6.5%), with similar proportions of positive (6.9%), neutral (7.2%) and negative (7.3%) invalid trials. All participants had at least 10 trials for each feedback type. To account for possible motion induced error that had not been solved by realignment and ARTrepair, we included six additional motion regressors (corresponding to the three translational and rotational directions) as covariates of no interest. The least squares parameter estimates of height of the best-fitting canonical HRF for each condition were used in pairwise contrasts. The pairwise comparisons resulted in subject-specific contrast images.

2.4.3. Higher-level group analyses

Subject-specific contrast images were used for the group analyses. Given that the all feedback > fixation baseline generally results in strong and robust activity, we validated our replication approach using this contrast (for results see Supplementary material). Our main analyses focus on the condition specific contrasts (e.g. 'positive vs. negative' feedback), using *t*-tests. Results were False Discovery Rate (FDR) cluster corrected ($pFDR < 0.05$), with a primary voxel-wise threshold of $p < 0.005$ (uncorrected) (Woo et al., 2014). Cluster-extend based thresholding has relatively high sensitivity (Smith and Nichols, 2009) and takes into account that individual voxel activations are not independent of the activations of voxels nearby (Heller et al., 2006). We set the primary p-value at $p < 0.005$ to strike the balance between too liberal cluster defining primary thresholds (e.g. $p < 0.01$; which can induce Type I errors) and more conservative primary thresholds (e.g. $p < 0.001$; which can induce Type II errors). Recently, cluster corrections have been debated for potential high Type I errors (Eklund et al., 2016), but the current three-sample design should reduce the risk for coincidental findings. Coordinates for local maxima are reported in MNI space.

2.4.4. Region of interest analyses

To extract patterns of activation in functionally defined clusters, SPM8's MarsBaR toolbox (Brett et al., 2002) was used. Besides ROIs derived from whole brain comparisons, we also performed analyses on three predefined ROIs based on adult social evaluation literature. These were the amygdala (from the Automated Anatomical Labeling (AAL) atlas (Tzourio-Mazoyer et al., 2002), left and right combined, center of mass (x,y,z) right: 27, −1, −19; left: −24, −2, −19), the anterior insula (from the conjunction contrast of Achterberg et al. (2016); left and right combined, center of mass (x,y,z) right: 34, 21, 0; left: −32, 20, −6) and the mPFC/ACCg (from the conjunction contrast of (Achterberg et al., 2016)), see Fig. 4a.

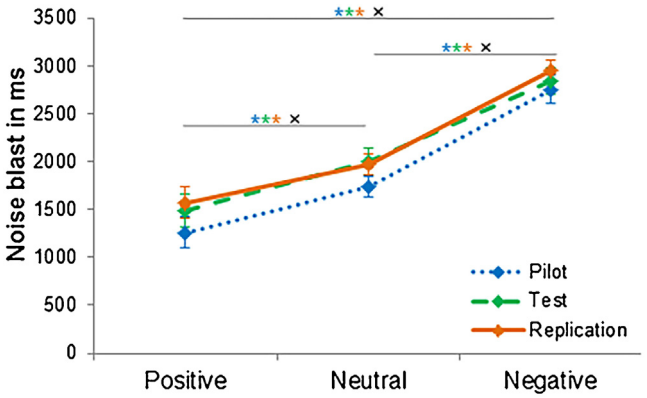

Fig. 2. Noise blast duration across the different social feedback conditions for the pilot, test, and replication sample. Error bars display standard error of mean. * significant differences for sample with matching color. × significant combined effect sizes in the meta-analysis.

Parameter estimates (PE, average Beta values) were extracted for the ROI analyses.

2.5. Statistical analyses

For noise blast duration, we first computed split-half reliability analyses. Positive, neutral and negative trials were randomly split in half and Pearson's correlation coefficients were calculated between both halves for each condition in all three samples. Split-half reliability analyses showed that the SNAT displayed excellent reliability in all three conditions: noise blast duration after positive (pilot: $r = 0.85$, test: $r = .96$, replication: $r = 0.96$; all p's < 0.001), neutral (pilot: $r = 0.83$, test: $r = 0.90$, replication: $r = .89$; all p's < 0.001) and negative social feedback (pilot: $r = 0.89$, test: $r = 0.94$, replication: $r = 0.84$; all p's < 0.001). Next, we used repeated measures ANOVA to investigate the noise blast duration after positive, neutral, and negative feedback in the three samples. Greenhouse-Geisser corrections were applied when the assumption of sphericitiy was violated. Pairwise comparisons were Bonferroni corrected. When outliers were detected (Z-value <−3.29 or >3.29), scores were winsorized (Tabachnick and Fidell, 2013). To compare the behavioral and neural effects over the different samples, we computed combined effect sizes using the Comprehensive Meta-Analysis (CMA) program (Borenstein et al., 2005).

3. Results

3.1. Behavioral results: noise blast duration

For each of the three samples (pilot, test, and replication) we performed a repeated measures ANOVA on noise blast duration after positive, negative, and neutral feedback. Results of the pilot sample showed a significant main effect of type of social feedback on noise blast duration, $F(2, 36) = 29.55$, $p < 0.001$, $\omega^2 = 0.46$, see Fig. 2. Pairwise comparisons revealed that noise blast duration after negative feedback ($M = 2718$ msec, $SD = 629$) in the pilot sample was significantly longer than noise blast duration after neutral feedback ($M = 1725$ msec; $SD = 470$, $p < 0.001$, $d = 1.78$), and after positive feedback (M = 1274 msec; $SD = 782$, $p < 0.001$, $d = 2.04$). Noise blast duration after neutral feedback was significantly longer than after positive feedback ($p = 0.007$, $d = 0.62$). These results were confirmed in the test sample ($F(2, 54) = 29.72$, $p < 0.001$, $\omega^2 = 0.30$). Participants in the test sample also gave significant longer noise blasts after negative feedback ($M = 2882$ msec; $SD = 790$), compared to neutral feedback ($M = 2024$ msec; $SD = 775$, $p < 0.001$, $d = 1.10$), and positive feedback (M = 1501 msec; $SD = 966$,

$p < 0.001$, $d = 1.57$). Noise blast duration after neutral feedback was also significantly longer than after positive feedback ($p < 0.001$, $d = 0.57$), see Fig. 2. A similar pattern was found in the replication sample ($F(2, 52) = 34.18$, $p < 0.001$, $\omega^2 = 0.39$). Participants in the replication sample also gave significant longer noise blast after negative feedback ($M = 2967$ msec; $SD = 573$) compared to neutral feedback ($M = 1967$ msec; SD = 636, $p < 0.001$, $d = 1.65$) and positive feedback (M = 1537 msec; $SD = 942$, $p < 0.001$, $d = 1.86$). Noise blast duration after neutral feedback was also significantly longer than after positive feedback ($p = 0.007$, $d = 0.50$), see Fig. 2.

To combine the results of the three different samples, we performed a meta-analysis. The difference between neutral and negative feedback showed a large combined effect size ($d = 1.41$, 95% confidence interval (CI): 0.97–1.84, $p < 0.001$). The difference between positive and negative feedback also showed a large combined effect size ($d = 1.74$, 95% CI: 1.19-2.29, $p < 0.001$). The combined effect for the difference between positive and neutral was medium in size ($d = 0.55$, 95% CI: 0.39–0.723, $p < 0.001$). Study outcomes were homogeneous; there was no heterogeneity in the results.

3.2. Neural activity: whole brain and ROI analyses

The general contrast (all feedback conditions vs. baseline) showed a robust pattern of activation. Most regions that were active in the pilot sample could be confirmed in the test sample, and all regions that were active in the test sample were replicated in the replication sample (see Supplementary materials). To test for differences between conditions, full factorial ANOVA's were performed that were then decomposed by pair-wise comparisons. Moreover, we performed exploratory whole brain analyses in the combined test and replication groups ($N = 55$), for which data were collected using the same MR scanner. Lastly, we performed ROI analyses in the three separate samples on three predefined ROIs: the amygdala (anatomically defined), the anterior insula and the mPFC/ACCg (based on Achterberg et al. (2016)). To combine the results, we performed meta-analyses across the three samples for each of these ROIs.

3.2.1. Whole brain condition effects per sample

3.2.1.1. Pilot sample. All significant pairwise comparisons are displayed in Table 2. The contrasts positive > negative and positive > neutral feedback both resulted in one cluster of heightened activation in the lateral occipital cortex. The contrast negative > neutral feedback resulted in two significant clusters: one in the left lateral occipital cortex and one in the left orbitofrontal cortex, extending into the left insula.

3.2.1.2. Test sample. All significant pairwise comparisons are displayed in Table 2. The contrasts positive > negative and positive > neutral feedback in the test sample also resulted clusters of heightened activation in the (lateral) occipital cortex. The contrast negative > neutral feedback resulted in two significant clusters, both in the lateral occipital cortex, extending into the fusiform gyrus.

3.2.1.3. Replication sample. All significant pairwise comparisons are displayed in Table 2. The contrasts positive > negative and positive > neutral feedback did not result in significant activation in the replication sample. Negative > positive feedback resulted in increased activation in the left inferior frontal gyrus, the left amygdala, and left lateral occipital cortex. Last, negative > neutral feedback resulted in increased activation of the left and right lateral occipital cortex, extending into the fusiform gyrus.

3.2.2. Whole brain condition effects in the combined test and replication samples

A full factorial ANOVA was computed based on the combined test and replication groups ($N = 55$). All significant pairwise comparisons are displayed in Table 3. The contrast negative > neutral and positive > neutral feedback resulted in heightened activation in the lateral occipital cortex. The contrast negative > positive feedback resulted in significant heightened activation in the right and left orbitofrontal cortex, the medial prefrontal cortex, the paracingulate gyrus, the left insula and the left superior temporal cortex (see Fig. 3a, Table 3). Fig. 3b presents a visual representation of mPFC activation after positive and negative social feedback for the combined test and replication group, as well as for the test and replication sample separately. The reversed contrast, positive > negative feedback did not resulted in any significant clusters.

3.2.3. ROI analyses in the three samples and combined effect sizes

3.2.3.1. Amygdala. Results for each of the three samples separately and the meta-analytic combination of results are displayed in Fig. 4b and Table 4. The pilot and replication samples showed significantly more amygdala activation after negative compared to positive feedback, but the test sample did not show an effect. The meta-analysis revealed that the difference in amygdala activation between negative and neutral feedback was not significant ($d = 0.21$, 95% CI: −0.12–0.54, $p = 0.204$). The combined effect size for the difference in amygdala activation between positive and neutral was also not significant ($d = 0.16$, 95% CI: −0.15–0.48, $p = 0.299$). However, the difference in amygdala activation between positive and negative feedback showed a significant combined effect size ($d = 0.47$, 95% CI: 0.09-0.84, $p = 0.015$), being larger for negative feedback. The study outcomes were homogeneous; there was no heterogeneity in the results.

3.2.3.2. Anterior insula. Results are displayed in Fig. 4c and Table 4. All samples showed increased anterior insula activation after negative *vs* neutral feedback, but the difference was only significant in the replication sample. The meta-analysis showed that the difference in anterior insula activation between negative and neutral feedback showed a significant combined effect size ($d = 0.40$, 95% CI: 0.11–0.69, $p = 0.007$), being larger for negative feedback. The combined effect size for the difference in anterior insula activation between positive and neutral was not significant ($d = 0.15$, 95% CI: −0.12–0.42, $p = 0.282$). Furthermore, the combined effect size for the difference in anterior insula activation between positive and negative feedback was not significant ($d = 0.24$, 95% CI: −0.06–0.53, $p = 0.123$). The study outcomes were homogeneous; there was no heterogeneity in the results.

3.2.3.3. Medial PFC/ACC gyrus. Results for each of the three samples separately are displayed in Fig. 4d and Table 4. Although the pattern of neural activation across conditions was similar to that of the anterior insula, there were no significant condition effects in the separate samples. However, the meta-analysis showed a significant combined effect size for the difference in mPFC/ACCg activation between negative and neutral feedback ($d = 0.33$, 95% CI: 0.01–0.66, $p = 0.045$), with more mPFC/ACCg activation after negative feedback. The combined effect size for the difference in mPFC/ACCg activation between positive and neutral feedback was in the expected direction (being larger for positive feedback) but not significant ($d = 0.22$, 95% CI: −0.03–0.46, $p = 0.080$). Furthermore, the combined effect size for the difference in mPFC/ACCg activation between positive and negative feedback was not significant ($d = 0.09$, 95% CI: −0.19–0.36, $p = 0.539$). The study outcomes were homogeneous; there was no heterogeneity in the results.

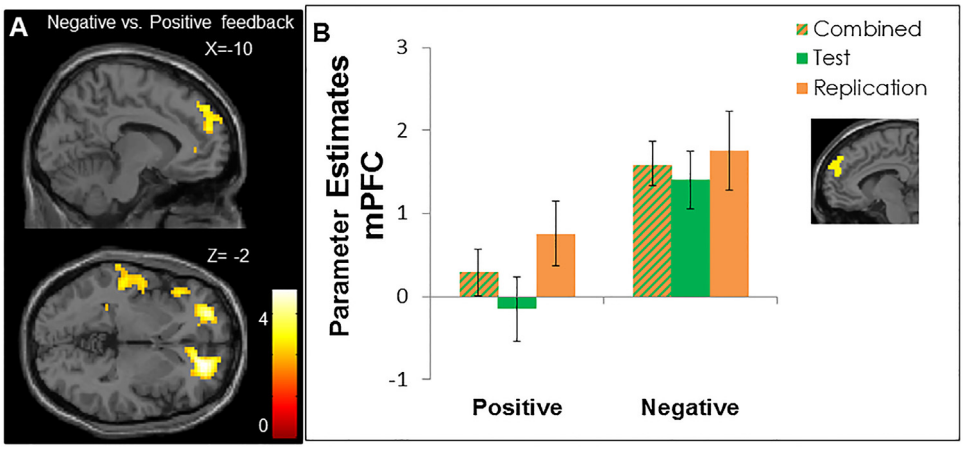

Fig. 3. a) whole brain results of the contrast negative vs. positive feedback in the test and replication samples combined ($N = 55$, $p < 0.005$, FDR cluster corrected). b) Mean parameter estimates for negative > positive feedback activation in the medial PFC cluster in the test and replication samples combined (N = 55, as displayed in Fig. 3A), as well as for the samples separately (center of mass (x,y,z): −1, 55, 31). Note that this graph is purely for visual representation and is not used for statistical inferences. Error bars indicate standard error of mean.

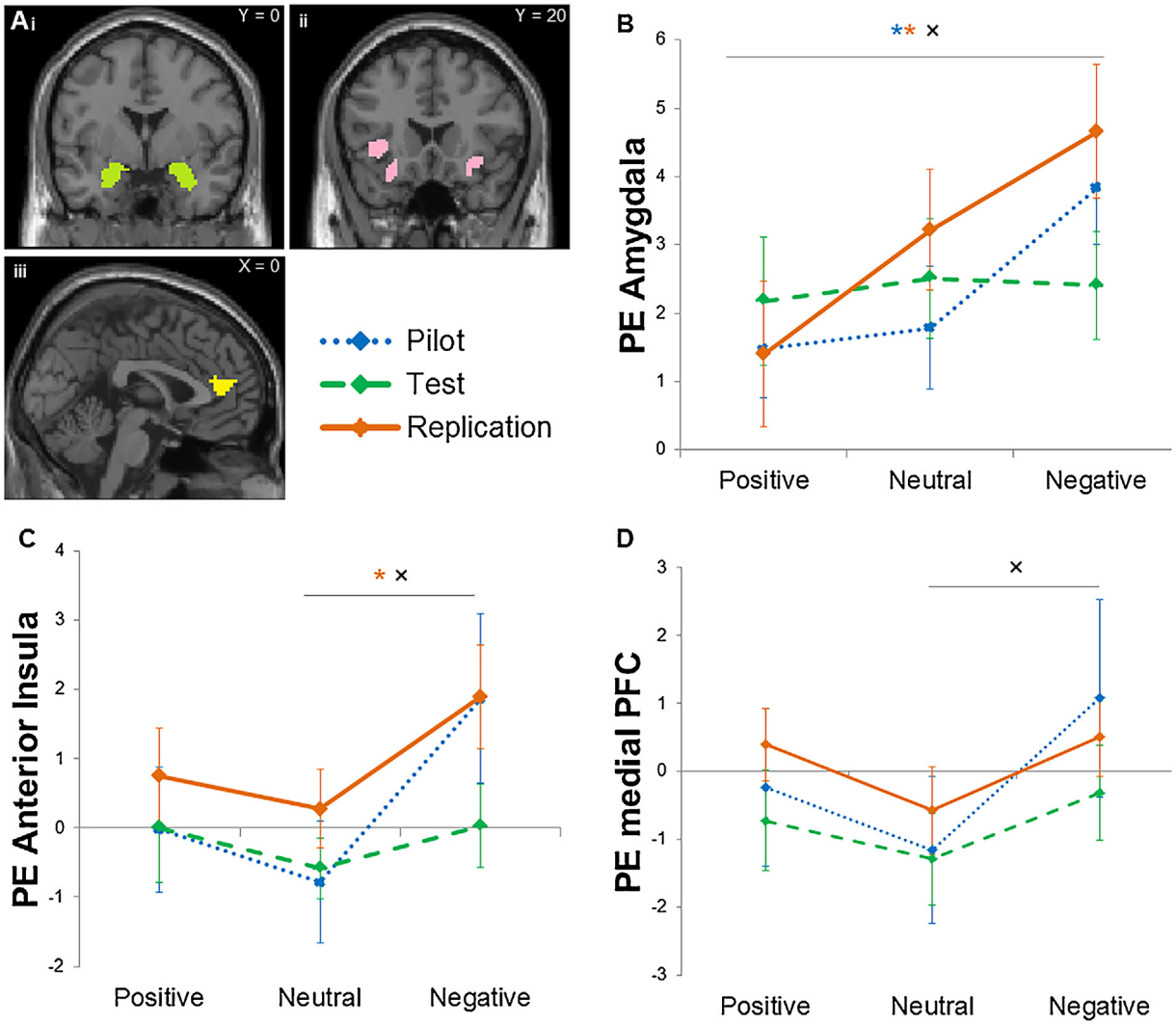

Fig. 4. a) visual representation of the ROIs: i) amygdala, ii) anterior insula and iii) medial PFC/ACC gyrus. Center of mass coordinates are presented in Section 2.4.4. b) Amygdala activation across the different social feedback conditions for the pilot, test, and replication sample. c) Anterior insula activation across the different social feedback conditions for the pilot, test, and replication sample. d) Medial PFC/ACC gyrus activation across the different social feedback conditions for the pilot, test, and replication sample. *significant difference for sample with matching color. × significant combined effect size in the meta-analysis. Error bars indicate standard error of mean.

Table 2
Whole brain condition effects per sample.

Area of Activation	Volume	*x*	*y*	*z*	*T*	*pFDR*
Pilot: positive > negative						
Lateral occipital cortex	649	3	−70	7	5.75	<0.001
Cuneal cortex		3	−76	25	5.03	
Supracalcarine cortex		0	−67	16	5.01	
Pilot: positive > neutral						
Lateral occipital cortex	2560	−45	−82	7	6.83	<0.001
Lingual gyrus		6	−67	4	6.43	
Lingual gyrus		18	−64	−2	6.22	
Pilot: negative > neutral						
Left lateral occipital cortex	348	−45	−82	7	5.04	<0.001
Left middle temporal gyrus		−51	−58	10	3.82	
Left lateral occipital gyrus		−39	−64	13	3.77	
Left orbitofrontal cortex	271	−36	23	−14	4.00	0.009
Left orbitofrontal cortex		−42	17	−14	3.90	
Left insula		−36	8	−5	3.86	
Test: positive > negative						
Lingual gyrus	337	−15	−88	−5	5.24	0.016
Lingual gyrus		9	−76	−5	4.30	
Occipital pole		−21	−94	−17	3.79	
Test: positive > neutral						
Occipital pole	1031	−15	−91	−5	6.17	<0.001
Occipital fusiform gyrus		24	−73	−5	5.96	
Lingual gyrus		9	−79	−5	5.36	
Test: negative > neutral						
Occipital pole	348	−6	−97	7	5.13	0.008
Lateral occipital cortex		−45	−85	4	4.13	
Lateral occipital cortex		−54	−79	4	3.84	
Lateral occipital cortex	274	48	−70	−5	3.86	0.013
Occipital fusiform gyrus		27	−73	−2	3.54	
Occipital fusiform gyrus		21	−82	−2	3.51	
Replication: positive > negative						
Left inferior frontal gyrus	325	−54	29	4	4.86	0.012
Left amygdala		−24	−1	−26	4.15	
Left frontal operculum cortex		−45	23	1	3.99	
Left lateral occipical cortex	402	−42	−79	4	4.38	0.008
Left lateral occipical cortex		−42	−76	22	3.71	
Lingual gyrus		−12	−57	−5	3.61	
Replication: neutral > positive						
Left precentral gyrus	1318	−15	−19	70	5.25	<0.001
Right precentral gyrus		27	−16	70	5.17	
Right precentral gyrus		9	−25	70	5.03	
Replication: neutral > negative						
Right precentral gyrus	293	30	−16	70	4.11	0.018
Left precentral gyrus		−9	−16	73	3.78	
Left precentral gyrus		−15	−22	79	3.37	
Replication: negative > neutral						
Left lateral occipital cortex	707	−42	−82	4	6.55	<0.001
Left lateral occipital cortex		−48	−73	−5	4.71	
Left occipital fusiform cortex		−39	−49	−14	4.36	
Left occipital pole	193	−12	−94	22	6.28	0.027
Left occipital pole		−6	−97	13	5.18	
Left lateral occipital cortex		−15	−85	40	3.53	
Right lateral occipital cortex	844	36	−76	−2	5.01	<0.001
Right lateral occipital cortex		48	−67	−2	4.97	
Right lateral occipital cortex		48	−76	4	4.85	

3.3. Brain-behavior correlations

Finally, we tested for brain-behavior correlations. Specifically, we correlated the meta-analytically significant brain results with noise blast duration. There were no significant results for negative > positive amygdala activation and aggressive behavior; nor for negative > neutral insula activation and aggression; nor for negative > neutral mPFC activation and aggression. Thus, we did not found significant brain-behavior relations, not in the samples separately, nor with a meta-analytical approach (see Supplementary materials).

4. Discussion

This study investigated the behavioral and neural correlates of social evaluation in middle childhood, using a new experimental paradigm: the Social Network Aggression Task (SNAT, Achterberg et al. (2016)). With the combination of a replication design and a meta-analytical approach we thoroughly tested this new experimental paradigm in 7-to-10-year-old children. Overall, we found consistent findings over the pilot, test and replication samples for behavioral aggression following negative social feedback, showing significantly more aggression after negative social feedback

Table 3
Whole brain condition effects combined test and replication sample.

Area of Activation	Volume	*x*	*y*	*z*	*T*	*pFDR*
Negative > neutral						
Left lateral occipital cortex	1080	−45	−82	4	6.90	<0.001
Left lateral occipital cortex		−6	−97	10	6.82	
Left occipital pole		−15	−94	22	5.93	
Right lateral occipital cortex	1053	48	−67	−5	6.10	<0.001
Right lateral occipital cortex		33	−76	−2	5.98	
Right occipital fusiform gyrus		18	−82	−2	5.60	
Positive > neutral						
Right occipital fusiform gyrus	1478	24	−73	−5	6.60	<0.001
Left occipital pole		−15	−91	−2	5.97	
Left occipital fusiform gyrus		−24	−76	−5	5.86	
Neutral > negative						
Right precentral gyrus	475	30	−13	67	4.21	0.002
Right middle frontal gyrus		33	14	43	4.19	
Right middle frontal gyrus		33	11	67	4.04	
Negative > positive						
Right orbitofrontal cortex	207	21	47	−2	4.94	0.039
Left orbitofrontal cortex	225	−27	50	−2	4.45	0.038
Left inferior frontal gyrus		−51	26	4	4.18	
Medial prefrontal cortex		−18	59	4	3.49	
Medial prefrontal cortex	259	−15	47	40	4.11	0.032
Medial prefrontal cortex		−6	62	31	4.07	
Paracingulate gyrus		−6	53	22	3.65	
Left insula	836	−45	−10	7	4.05	<0.001
Left parietal operculum cortex		−30	−34	22	3.99	
left superior temporal cortex		−54	−4	7	3.85	

compared to positive or neutral social feedback The neural effects indicated increased activity in the amygdala, insula and mPFC/ACCg after negative feedback, but these effects were only significant in part of the samples and in the meta-analyses. The specific social evaluation effects and methodological considerations for future research are described in more detail below.

4.1. Social evaluation in childhood

The SNAT showed reliable and consistent behavioral results, with stronger behavioral aggression (noise blast duration) after social rejection. The meta-analysis showed medium to (very) large combined effect sizes over the three samples. This study complements the large number of prior studies that focused mainly on withdrawal, as we showed that social rejection feedback also elicits aggression in children. This is in line with previous results in adults (Achterberg et al., 2016), suggesting that children make similar distinctions between social evaluation as adults do. Moreover, these results are consistent with questionnaire studies that show more (teacher reported) aggression after social rejection in children (Dodge et al., 2003; Nesdale and Lambert, 2007; Lansford et al., 2010).

The next question concerned whether neural activation differed depending on whether the participant received positive, neutral or negative social feedback. The separate samples did show the same significant condition effects. In the pilot sample, we found significant heightened activation in the insula after negative vs. neutral social feedback, similar to the effects reported in adults (Achterberg et al., 2016). However, whole brain analyses did not reveal this effect in the test or replication samples. Moreover, although heightened activation in the visual cortex (including the fusiform gyrus) after positive compared to negative and neutral feedback was consistent over the pilot and test sample, we could not confirm this in the replication sample. Our relatively small samples (with sample sizes ranging between n = 19 and n = 28) might not have had sufficient power to detect robust condition effects in whole brain analyses.

In the larger combined sample (including twin siblings, $N = 55$) rejection feedback was associated with increased activity in mPFC. This region borders the mPFC/ACCg region observed in adults, with increased activity in response to negative and positive feedback (Achterberg et al., 2016). Indeed, an ROI analysis of this mPFC/ACCg region based on the adult study (Achterberg et al., 2016) confirmed elevated activity after rejection in children. A recent review on the ACC and social cognition (Apps et al., 2016) describes an anatomical and function subdivision between the anterior cingulate cortex' sulcus and gyrus. The region described as the ACC gyrus (ACCg; located adjacent and dorsal to the genu of the corpus callosum in humans) shows overlap with the region that showed increased activation after negative social feedback in children (this study) and for general social evaluation in adults (Achterberg et al., 2016). The ACCg region has been suggested to be sensitive to factors determining the others' motivation (see Apps et al. (2016)). Moreover, the meta-analysis showed that the anterior insula was more active after negative compared to neutral feedback, which is in line with the results reported in adults (Achterberg et al., 2016). The anterior insula has been shown to have strong connections (both structurally as functionally) with this ACCg region (Apps et al., 2016) and several neuroimaging studies have pointed towards the anterior insula and midline areas of the brain as important brain regions responding to social rejection (for meta-analysis see Cacioppo et al. (2013), Rotge et al. (2015)).

In addition, the meta-analysis showed significantly more activation in the amygdala after negative feedback compared to positive feedback. A recent cross-sectional study of 112 participants with ages ranging from 6 to 23 years showed decreased amygdala reactivity over age, suggesting a shift from bottom-up amygdala based processing to a more top-down processing in adolescence and adulthood (Silvers et al., 2016). That study focused on the processing of negative and positive scenes and showed strongest reactivity for emotional scenes in general (independent of valence) in younger participants. This may indicate that the amygdala serves as an important region for processing affectively salient stimuli in childhood in particular. An interesting question for future research is to examine how amygdala response to social feedback relates to

Table 4
Comprehensive Meta-Analyses of the condition effects.

		d	95% CI lower limit	95% CI upper limit
Amygdala				
Negative > Positive	Pilot	0.70*	0.06	1.34
	Test	0.05	−0.52	0.62
	Replication	0.61**	0.20	1.02
	Meta	*0.47**	*0.09*	*0.84*
Negative > Neutral	Pilot	0.54	−0.05	1.14
	Test	−0.02	−0.41	0.36
	Replication	0.30	−0.22	0.81
	Meta	*0.21*	*−0.12*	*0.54*
Neutral > Positive	Pilot	0.09	−0.52	0.69
	Test	0.07	−0.42	0.55
	Replication	0.36	−0.20	0.91
	Meta	*0.17*	*−0.15*	*0.48*
Anterior Insula				
Negative > Positive	Pilot	0.40	−0.29	1.09
	Test	0.06	−0.44	0.55
	Replication	0.31	−0.14	0.75
	Meta	*0.24*	*−0.06*	*0.53*
Negative > Neutral	Pilot	0.57	−0.08	1.21
	Test	0.22	−0.28	0.72
	Replication	0.46*	0.03	0.90
	Meta	*0.40***	*0.11*	*0.69*
Positive > Neutral	Pilot	0.20	−0.30	0.07
	Test	0.11	−0.32	0.55
	Replication	0.14	−0.34	0.62
	Meta	*0.15*	*−0.12*	*0.42*
Medial Prefrontal Cortex				
Negative > Positive	Pilot	0.23	−0.45	0.90
	Test	0.11	−0.46	0.67
	Replication	0.04	−0.32	0.40
	Meta	*0.09*	*−0.19*	*0.36*
Negative > Neutral	Pilot	0.40	−0.30	1.10
	Test	0.27	−0.32	0.86
	Replication	0.34	−0.12	0.81
	Meta	*0.33**	*0.01*	*0.66*
Positive > Neutral	Pilot	0.19	−0.31	0.68
	Test	0.15	−0.22	0.52
	Replication	0.32	−0.10	0.73
	Meta	*0.22*	*−0.03*	*0.46*

* $p < 0.05$.
** $p < 0.01$.

social behavior in childhood and how it unfolds over time during childhood and adolescence.

Interestingly, in the meta-analyses, we did not find significantly more activation in any of the regions after positive feedback (compared to neutral feedback), which is not in line with previous adult findings (Achterberg et al., 2016) or with prior studies that focused on adolescents using similar paradigms (Gunther Moor et al., 2010; Silk et al., 2012b). Positivity biases are thought to be larger in childhood than in adolescence or adulthood (Mezulis et al., 2004), possibly indicating that children have a stronger belief that they will be positively evaluated by others. This may result in more salience of neutral or negative feedback relative to positive feedback. Thus, although we found that behaviorally children reacted in a similar way to social evaluation as adults do, the similarities in neural findings between children and adults are more mixed. The neural signature of social rejection in terms of anterior insula and mPFC/ACCg activation was found to be present in middle childhood, but it was less pronounced than in adults (only detectable in larger samples and meta-analysis). This was the first study to test whether children engage similar brain regions in processing social evaluation as adults. By using various approaches (whole brain analyses, three different samples, meta-analysis) we had the opportunity to investigate these regions in detail. However, there are several methodological considerations that follow from the current study.

4.2. Methodological considerations

First, whole brain analyses in this age range may need larger samples, since the use of fMRI in children is more affected by motion (O'Shaughnessy et al., 2008), but also because there is substantial individual variation in the timing of brain maturation (Pfeifer and Allen, 2016). Some of our independent (one sample) ROI analyses did not show significant effects, while meta-analytically combining the results did reveal significant effects (see for similar results Scheibehenne et al. (2016)). This highlights the importance not only of internal replication but also of incorporating a meta-analytical approach. By applying meta-analysis in the context of one study testing a paradigm in different subsamples, we can minimize the risk that meta-analytic results in the (broader) field of neuroimaging studies are distorted due to publication bias (i.e., the bias resulting from selective publication of significant results (Franco et al., 2014)).

The current study is the first neuroimaging study to use both a replication and meta-analytical approach to test a new experimental paradigm in children. Our test and replication sample consisted

of same-sex twin pairs of which the first and second born twin were randomly assigned to one of the two samples. Therefore these samples are not independent, which could result in more equivalent results. However, additional meta-analyses in which we treated the test and replication samples as if they consisted of the same participants (which is too conservative), and then combined the effect size with the effect size of the pilot sample, showed similar combined effect-sizes, with somewhat larger confidence intervals due to the lower N. Moreover, for an exact replication this can be considered an advantage as it reduces the influence of third variables (for example when the replication sample is older or more intelligent), and methodologically this type of replicability is considered one of the important cornerstones of science (Van IJzendoorn, 1994; Gabrieli et al., 2015). Nevertheless, this does have implications for the whole brain analyses with the test and replication samples combined. These are exploratory, and the results need to be confirmed in future larger and independent samples.

Ultimately, results of different, but comparable, social evaluation paradigms in children should be combined to unravel the neural underpinnings of social evaluation in a developmental perspective. Moreover, although the current study shows increased aggression and increased neural activation after rejection, we could not identify significant brain-behavior correlations, probably due to our limited sample sizes. Nevertheless, these individual differences in brain activation during social evaluation in children could be informative, as we recently showed that individual differences in dorsal lateral PFC activation during social evaluation in adults was related to individual differences in behavioral aggression (Achterberg et al., 2016). Future studies should include larger developmental samples to investigate these associations, and explore why some children react with more aggression after negative social feedback than others.

5. Limitations

In addition to the methodological considerations, some limitation regarding the social evaluation paradigm used in this study need to be acknowledged. First, although the noise blast is often used as a measure of aggression, our cover story explicitly stated that the peers would not hear the noise blast. That is to say, the aggression measure reflects hypothetical aggression or frustration. This decision was based on previous studies using a similar design (Konijn et al., 2007), but future studies may separate real aggression from hypothetical aggression to test the neural differences in these two types of aggression. Secondly, our social evaluation paradigm included a neutral condition. However, our neutral feedback was not purely neutral, but more mixed (not specifically positive and not specifically negative). Nevertheless, the neutral condition was in between positive and negative feedback, therefore making this condition a solid baseline/comparison condition.

6. Conclusion

Using both a replication and a meta-analytical approach, we showed that the Social Network Aggression Task reveals robust and reliable behavioral results. Negative social feedback resulted in the highest levels of behavioral aggression. Moreover, meta-analyses on predefined ROIs revealed that negative social feedback resulted in more neural activation in the amygdala (compared to positive feedback) and in the anterior insula and mPFC/ACCg (compared to neutral feedback). Exploratory whole brain analyses confirmed heightened activation in the medial prefrontal cortex (mPFC) after negative relative to neutral social feedback. Future research should examine how neural responses to social feedback and subsequent aggression are related, using larger samples that allow for testing correlates of individual differences in aggression after negative social feedback. The current findings show that the Social Network Aggression Task is a reliable paradigm for the investigation of social evaluation and aggression in children, and indicate that this paradigm is feasible for use in larger and longitudinal developmental studies.

Conflict of interest

The authors declare no competing financial interest.

Acknowledgements

The Leiden Consortium on Individual Development is funded through the Gravitation program of the Dutch Ministry of Education, Culture, and Science and the Netherlands Organization for Scientific Research (NWO grant number 024.001.003).

Appendix A. Supplementary data

Supplementary data associated with this article can be found, in the online version, at http://dx.doi.org/10.1016/j.dcn.2017.02.007.

References

Achterberg, M., van Duijvenvoorde, A.C., Bakermans-Kranenburg, M.J., Crone, E.A., 2016. Control your anger! The neural basis of aggression regulation in response to negative social feedback. Soc. Cogn. Affect. Neurosci. 11 (5), 712–720.
Apps, M.A., Rushworth, M.F., Chang, S.W., 2016. The anterior cingulate gyrus and social cognition: tracking the motivation of others. Neuron 90 (4), 692–707.
Berndt, T.J., 2004. Children's friendships: shifts over a half-century in perspectives on their development and their effects. Merrill-Palmer Q.-J. Dev. Psychol. 50 (3), 206–223.
Borenstein, M., Rothstein, D., Cohen, J., 2005. Comprehensive meta-analysis: a computer program for research synthesis. NJ: Biostat.
Brett, M., Anton, J.L., Valabregue, R., Poline, J.B., (2002) 'Region of interest analysis using an SPM toolbox [abstract] Presented at the 8th International Conference on Functional Mapping of the Human Brain, June 2-6', Available on CD-ROM in NeuroImage, 16(2).
Cacioppo, S., Frum, C., Asp, E., Weiss, R.M., Lewis, J.W., Cacioppo, J.T., 2013. A quantitative meta-analysis of functional imaging studies of social rejection. Sci. Rep. 3.
Chester, D.S., Eisenberger, N.I., Pond Jr., R.S., Richman, S.B., Bushman, B.J., Dewall, C.N., 2014. The interactive effect of social pain and executive functioning on aggression: an fMRI experiment. Soc. Cogn. Affect. Neurosci. 9 (5), 699–704.
Dale, A.M., 1999. Optimal experimental design for event-related fMRI. Hum. Brain Mapp. 8 (2–3), 109–114.
Dodge, K.A., Lansford, J.E., Burks, V.S., Bates, J.E., Pettit, G.S., Fontaine, R., Price, J.M., 2003. Peer rejection and social information-processing factors in the development of aggressive behavior problems in children. Child Dev. 74 (2), 374–393.
Eklund, A., Nichols, T.E., Knutsson, H., 2016. Cluster failure: why fMRI inferences for spatial extent have inflated false-positive rates. Proc. Natl. Acad. Sci. U. S. A. 113 (28), 7900–7905.
Flagan, T., Beer, J.S., 2013. Three ways in which midline regions contribute to self-evaluation. Front. Hum. Neurosci. 7, p450.
Franco, A., Malhotra, N., Simonovits, G., 2014. Publication bias in the social sciences: unlocking the file drawer. Science 345 (6203), 1502–1505.
Gabrieli, J.D.E., Ghosh, S.S., Whitfield-Gabrieli, S., 2015. Prediction as a humanitarian and pragmatic contribution from human cognitive neuroscience. Neuron 85 (1), 11–26.
Gunther Moor, B., van Leijenhorst, L., Rombouts, S.A., Crone, E.A., Van der Molen, M.W., 2010. Do you like me? Neural correlates of social evaluation and developmental trajectories. Soc. Neurosci. 5 (5–6), 461–482.
Guyer, A.E., Lau, J.Y., McClure-Tone, E.B., Parrish, J., Shiffrin, N.D., Reynolds, R.C., Chen, G., Blair, R.J., Leibenluft, E., Fox, N.A., Ernst, M., Pine, D.S., Nelson, E.E., 2008. Amygdala and ventrolateral prefrontal cortex function during anticipated peer evaluation in pediatric social anxiety. Arch. Gen. Psychiatry 65 (11), 1303–1312.
Guyer, A.E., Caouette, J.D., Lee, C.C., Ruiz, S.K., 2014. Will they like me? Adolescents' emotional responses to peer evaluation. Int. J. Behav. Dev. 38 (2), 155–163.
Heller, R., Stanley, D., Yekutieli, D., Rubin, N., Benjamini, Y., 2006. Cluster-based analysis of FMRI data. Neuroimage 33 (2), 599–608.
Konijn, E.A., Bijvank, M.N., Bushman, B.J., 2007. I wish I were a warrior: the role of wishful identification in the effects of violent video games on aggression in adolescent boys. Dev. Psychol. 43 (4), 1038–1044.

Lansford, J.E., Malone, P.S., Dodge, K.A., Pettit, G.S., Bates, J.E., 2010. Developmental cascades of peer rejection, social information processing biases, and aggression during middle childhood. Dev. Psychopathol. 22 (3), 593–602.
Masten, C.L., Eisenberger, N.I., Borofsky, L.A., Pfeifer, J.H., McNealy, K., Mazziotta, J.C., Dapretto, M., 2009. Neural correlates of social exclusion during adolescence: understanding the distress of peer rejection. Soc. Cogn. Affect. Neurosci. 4 (2), 143–157.
Mazaika, P.K., Hoeft, F., Glover, G.H., Reiss, A.L., 2009. Methods and software for fMRI analyses for clinical subjects. In: Human Brain Mapping Conference, San Francisco, CA.
Mezulis, A.H., Abramson, L.Y., Hyde, J.S., Hankin, B.L., 2004. Is there a universal positivity bias in attributions? A meta-analytic review of individual, developmental, and cultural differences in the self-serving attributional bias. Psychol. Bull. 130 (5), 711–747.
Nesdale, D., Lambert, A., 2007. Effects of experimentally manipulated peer rejection on children's negative affect, self-esteem, and maladaptive social behavior. Int. J. Behav. Dev. 31 (2), 115–122.
Nolan, S.A., Flynn, C., Garber, J., 2003. Prospective relations between rejection and depression in young adolescents. J. Pers. Soc. Psychol. 85 (4), 745–755.
O'Shaughnessy, E.S., Berl, M.M., Moore, E.N., Gaillard, W.D., 2008. Pediatric functional magnetic resonance imaging (fMRI): issues and applications. J. Child Neurol. 23 (7), 791–801.
Open Science, C., 2015. PSYCHOLOGY. Estimating the reproducibility of psychological science. Science 349 (6251), p. aac4716.
Pfeifer, J.H., Allen, N.B., 2016. The audacity of specificity: moving adolescent developmental neuroscience towards more powerful scientific paradigms and translatable models. Dev. Cogn. Neurosci. 17, 131–137.
Riva, P., Romero Lauro, L.J., DeWall, C.N., Chester, D.S., Bushman, B.J., 2015. Reducing aggressive responses to social exclusion using transcranial direct current stimulation. Soc. Cogn. Affect. Neurosci. 10 (3), 352–356.
Rotge, J.Y., Lemogne, C., Hinfray, S., Huguet, P., Grynszpan, O., Tartour, E., George, N., Fossati, P., 2015. A meta-analysis of the anterior cingulate contribution to social pain. Soc. Cogn. Affect. Neurosci. 10 (1), 19–27.
Scheibehenne, B., Jamil, T., Wagenmakers, E.J., 2016. Bayesian evidence synthesis can reconcile seemingly inconsistent results: the case of hotel towel reuse. Psychol. Sci. 27 (7), 1043–1046.
Siegle, G.J., Steinhauer, S.R., Carter, C.S., Ramel, W., Thase, M.E., 2003. Do the seconds turn into hours? Relationships between sustained pupil dilation in response to emotional information and self-reported rumination. Cogn. Therapy Res. 27 (3), 365–382.
Silk, J.S., Stroud, L.R., Siegle, G.J., Dahl, R.E., Lee, K.H., Nelson, E.E., 2012a. Peer acceptance and rejection through the eyes of youth: pupillary, eyetracking and ecological data from the Chatroom Interact task. Soc. Cogn. Affect. Neurosci. 7 (1), 93–105.
Silk, J.S., Stroud, L.R., Siegle, G.J., Dahl, R.E., Lee, K.H., Nelson, E.E., 2012b. Peer acceptance and rejection through the eyes of youth: pupillary, eyetracking and ecological data from the Chatroom Interact task. Soc. Cogn. Affect. Neurosci. 7 (1), 93–105.
Silk, J.S., Siegle, G.J., Lee, K.H., Nelson, E.E., Stroud, L.R., Dahl, R.E., 2014. Increased neural response to peer rejection associated with adolescent depression and pubertal development. Soc. Cogn. Affect. Neurosci. 9 (11), 1798–1807.
Silvers, J.A., Insel, C., Powers, A., Franz, P., Helion, C., Martin, R., Weber, J., Mischel, W., Casey, B.J., Ochsner, K.N., 2016. The transition from childhood to adolescence is marked by a general decrease in amygdala reactivity and an affect-specific ventral-to-dorsal shift in medial prefrontal recruitment. Dev Cogn Neurosci.
Smith, S.M., Nichols, T.E., 2009. Threshold-free cluster enhancement: addressing problems of smoothing, threshold dependence and localisation in cluster inference. Neuroimage 44 (1), 83–98.
Somerville, L.H., Heatherton, T.F., Kelley, W.M., 2006. Anterior cingulate cortex responds differentially to expectancy violation and social rejection. Nat. Neurosci. 9 (8), 1007–1008.
Tabachnick, B., Fidell, S., 2013. Using Multivariate Statistics, 6th ed. Pearson, Boston.
Thomaes, S., Stegge, H., Olthof, T., Bushman, B.J., Nezlek, J.B., 2011. Turning shame inside-out: humiliated fury in young adolescents. Emotion 11 (4), 786–793.
Tzourio-Mazoyer, N., Landeau, B., Papathanassiou, D., Crivello, F., Etard, O., Delcroix, N., Mazoyer, B., Joliot, M., 2002. Automated anatomical labeling of activations in SPM using a macroscopic anatomical parcellation of the MNI MRI single-subject brain. Neuroimage 15 (1), 273–289.
Van IJzendoorn, M.H., 1994. Process model of replication studies: on the relations between different types of replication. In: van der Veer, R., Van IJzendoorn, M.H., Valsiner, J. (Eds.), On Reconstructing the Mind. Replicability in Research on Human Development. Ablex Norwood, NJ.
Woo, C.W., Krishnan, A., Wager, T.D., 2014. Cluster-extent based thresholding in fMRI analyses: pitfalls and recommendations. Neuroimage 91, 412–419.